Load Decomposition at Smart Meters Level Using Eigenloads Approach

Hamed Ahmadi, *Student Member, IEEE*, and José R. Martí, *Fellow, IEEE*

***Abstract*—The deployment of the advanced metering infrastructure (AMI) in distribution systems provides an excellent opportunity for load monitoring applications. Load decomposition can be done at the smart meters level, providing a better understanding of the load behavior at near-real-time. In this paper, loads' current and voltage waveforms are processed off-line to form a comprehensive library. This library consists of a set of measurements projected onto the *eigenloads* space. Eigenloads are basically the eigenvectors describing the *load signatures* space. Similar to human faces, every load has a distinct signature. Each load measurement is transformed into a *photo* and an efficient face recognition algorithm is applied to the set of photos. A list of all the on-line devices is always stored and can be accessed at any time. The proposed method can be implemented at the smart meters level. The distributed computation that can be achieved by performing simple calculations at each smart meter, without the need for sending intensive data to a central processor, is beneficial. From a system operator perspective, load composition in near-real-time provides the loads' voltage dependence that are needed, for example, in Volt-VAR Optimization (VVO) in distribution systems. Further applications of load composition data are also discussed.**

***Index Terms*—Load decomposition, principal component analysis, *S* transform.**

I. Introduction

THE modern distribution management system (DMS) offers a variety of useful applications in distribution systems. The main functions of a typical DMS include state estimation, load allocation, power flow analysis, volt-VAR optimization (VVO), load shedding, fault management, system restoration, feeder reconfiguration, load forecasting, etc. Although these capabilities are appealing, they usually need continuous monitoring of the system and real-time measurements. Fortunately, the deployment of advanced metering infrastructure (AMI) provides the opportunity for the effective application of DMS.

One of the most important features of distribution systems is the load behavior, which is also the main source of change in the state of the system during normal conditions. A thorough understanding of the load nature can make an important impact on the performance of a control action in the system. In a particular case, in order to successfully manage the voltage and reactive power (VAR) in a system via VVO, the load voltage dependencies are the main factors since the voltage level affects the active and reactive power consumptions. In order to reach a high level of accuracy in the load voltage dependency modeling, the load composition at each node is needed. Since the measurements are usually provided in a composite form, decomposition techniques are required to recognize the individual load components and their expected behavior.

This work was supported by the Natural Science and Engineering Research Council (NSERC) of Canada. The authors are with the Department of Electrical and Computer Engineering, University of British Columbia, Vancouver, BC, V6T 1Z4, Canada (e-mail: hameda@ece.ubc.ca; jrms@ece.ubc.ca).

A. Problem Statement

Electricity is brought to a customer through a supply point, where the utility meter connects the customer to the grid. All the possible measurements by the utility happen at the meter level, and no further access is available beyond this point. Since the measured quantities (e.g., current and power) are an aggregate of the total consumption of the customer, further analysis is required to decompose the measured data into its components. For example, a residential customer may have a variety of loads, such as lights, refrigerators, heaters, electronics, etc., connected at the same time. It is, however, a challenge to retrieve this information from the aggregate measurement at the meter.

The measurements at the substations are an aggregation of a very large number of different loads and, practically speaking, it is not feasible to find an accurate composition at this level. The lowest level of measurement points is the smart meters, where the current (I), voltage (V), active/reactive power (P/Q), and power factor (PF) can be measured by some sampling rate. The important challenge in the load decomposition process is to define "features" that: 1) can be easily extracted from the measured data; 2) provide a basis to distinguish between different loads. Every family of loads has distinct features that make it different from others. For instance, ideal resistive loads have no harmonics, no inrush current, and unity PF, while induction motor loads may have the third harmonic, an inrush current, and a non-unity PF. Another challenge is to distinguish between loads with similar *features* but different applications. For instance, a large incandescent light and a small iron may have similar *features*, while they have totally different applications.

B. Proposed Approach

In this paper, apparent power is taken as the loads' feature. A time-frequency transformation is then applied to the time-domain measurements to form a set of *photos* for loads, defining their identities. The principal component analysis (PCA) is then applied to the set of photos to extract the important features, called "eigenloads". This idea was previously applied to personal photos of different people in [1] to find *eigenfaces*. Based on the calculated eigenloads, each load signature can be expressed as a vector of weights, indicating the contribution of each eigenload. This provides a simple process to compare

different load signatures and determine their similarities in a quantitative way. Besides its mathematical sense, the eigenload approach has physical interpretations as well in categorizing the loads into several groups, each with distinct features.

C. Related Literature

The concept of load disaggregation was first used in the early 80's for load forecasting purposes [2]. Many studies have been conducted for load disaggregation using different techniques and/or different load features. To characterize the load signature, the plots of active power P versus reactive power Q have been used in [3], which was commercialized under a nonintrusive appliance load monitoring system (NIALMS) [4]. An improved version of this method was proposed in [5] taking into account the harmonic contents of the signals, which addresses one of the inadequacies of NIALMS. A voltage-current (V-I) trajectory was used as the load signature in [6] which has shown good performance in distinguishing between loads with similar patterns. A deeper vision of the V-I trajectory for load identification was introduced in [7], which improved the precision of predictions by 10% as compared to [6]. The features used in [7] include P-Q, total harmonic distortion, and V-I wave-shape. Four learning algorithms were also used in [7], including Artificial Neural Network (ANN), ANN coupled with an evolutionary algorithm, Support Vector Machine (SVM), and Adaptive Boost. It was shown that the Adaptive Boost algorithm based on I-V wave-shape produces the highest accuracy in the predictions. The Wavelet transform (WT) was utilized in [8] to decompose the measured signals into time and frequency domains. Using a sampling frequency of 10 kHz, current waveforms were decomposed into 6 WT components. This WT decomposition, similar to Fourier decomposition of time series, can be used to classify loads.

A thorough survey on the available methods for load disaggregation was done in [9]. Based on this study, the data available from the smart meters have a high potential to be useful for load disaggregation purposes. The utilization of smart meters data for load disaggregation has been recently reported, for example, in [10] and [11]. The smart meter data was utilized in [10] and an Explicit-Duration Hidden-Markov Model with differential observations was applied to the data for detecting and estimating individual home appliance loads. An event window-based mechanism was proposed in [11] which uses the power waveforms and clusters the signatures based on some features in a selected time window. A real-time load monitoring approach was introduced in [12] which is based on ANN and uses P, Q, PF, peak and RMS values of V and I.

The SVM algorithm as well as 5-Nearest Neighbors method were employed in [13] to classify loads using P, Q, and PF data. An algorithm was proposed in [14] to recognize major appliances in a household, namely water heater, baseboard heater, washing machine, and refrigerator, which only uses P as the feature to classify loads. When two loads have similar power consumption, the algorithm in [14] may fail. A pattern recognition approach was introduced in [15] to decompose the energy use of major appliances in a household using P measurements. This method needs an on-site training for the first time for about a week and it will work as long as no new appliance is added. A few possible load configurations can be found using the algorithm proposed in [16], which utilizes P and Q signals and applies a finite-state machine based on fuzzy transitions to classify loads. In an experiment, the method in [16] found two possible configurations, one of which was the correct one.

There are research groups worldwide concentrating on developing load disaggregation techniques. The research group at Jin Wen University of Science and Technology in Taiwan has recently published the results of their work based on multiple algorithms, such as ANN [17], Particle Swarm Optimization (PSO) [18], and WT [19]. The results of their study have shown noticeable recognition rates. The problem of load disaggregation was well described in [20] and [21]. Different load features such as I, P, Q, harmonics, instantaneous admittance waveform, instantaneous power waveform, eigenvalues, and switching transient waveform were used. Two disaggregation algorithms were also proposed based on optimization or pattern recognition (based on ANN). A *committee decision mechanism* was then adopted to render the best solution out of a *candidate pool* containing candidates obtained by different features. This framework has shown good performance in terms of accuracy of the estimations.

Table I provides a summary of the specifications of some of the reviewed research on the subject of load disaggregation. This table is a good reference for comparing these studies in terms of the adopted methodologies, load features, sampling rates in data acquisition, and success rate in the recognition.

D. Objectives

Most of the aforementioned research work on load disaggregation require relatively high computational efforts in the recognition process. To this end, the measured data needs to be sent to a central processor on which the optimization algorithms can be run. It is desirable, however, to be able to implement the disaggregation algorithm at the smart meter level and just transfer the results using the limited communication capabilities of the current smart meter infrastructure. This requires a low-computation algorithm that can be implemented using microprocessors and low-capacity memory storage located in the smart meter or in a box next to it. The aim of this paper is to develop a methodology that satisfies those requirements.

The main idea in this study is to characterize the load signature, i.e. its current and/or voltage waveforms, in a way that is easily distinguishable. To achieve this goal, the concept of *eigenloads* is introduced. The eigenloads are, similar to the eigenvalues concept, the basic building blocks that can be used to reproduce all load signatures. This idea has been previously used in the well-cited paper by Turk and Pentland [1] for face recognition. Some electric devices draw a transient current which varies over a period of time, e.g., a motor load draws a current equal to several multiples of its steady state value during the starting period. Therefore, a time-frequency analysis is required to capture the full signature of a particular load.

Table I
SPECIFICATIONS SUMMARY OF THE LITERATURE ON LOAD DISAGGREGATION

Reference	Load Features	Techniques	Sampling Rate	Success Rate
[3],[4]	P,Q, ON/OFF duration	Finite State Machine	7.7 kHz	0-100%
[7]	V-I wave-shape	Adaptive Boost	16.5 kHz	> 90%
[11]	$P(t)$	Edge, Sequence, Trend, and Time signatures	N/A	> 90%
[12]	P, Q, PF, RMS and peak of V and I	ANN	1/60 Hz	> 84%
[13]	P, Q, PF	SVM, 5-Nearest Neighbors	2.5 Hz	> 95%
[15]	P	Pattern recognition	1/16 Hz	>84%
[17]	Turn-on transient energy	ANN	15.4 kHz	>39%
[18]	P, Q	ANN, PSO	6 kHz	>92%
[19]	WT of I	ANN	15 kHz	> 90%

Using a time-frequency transformation, each measurement can be transformed into a *photo* representing the particular load, which opens the path for applying well-developed face recognition mechanisms to the load identification problem without the need for sophisticated optimization algorithms.

The rest of the paper is organized as follows. In Section II, the methodology used in this paper is described. The results of applying the proposed approach to real laboratory measurements are presented in Section III. The applications, limitations, and implementation aspects of the proposed method are discussed in Section IV. The main findings of this study are summarized in Section V.

II. METHODOLOGY

The first step in load decomposition is to collect measurements, i.e. the current and voltage waveforms. The instantaneous power is chosen as the load signature. The waveform of the current by itself may not give enough features to distinguish among loads since it does not account for the power factor (phase shift between voltage and current waveforms). The instantaneous power $s(t)$ is the multiplication of current and voltage signals and, therefore, contains informations about power factor (see Section IV-A). In order to extract the frequency contents of $s(t)$, a suitable transformation is required.

A. Time-Frequency Representation

During the transient period after load connection, each load draws a current with different frequency contents for different durations. This means that a fixed-window transformation, such as the Fourier Transform, is not useful to accurately represent load identities. To take this into account, the authors suggest the use of the family of time-frequency transformations that provide the frequency contents of a signal over time. There are some transformations that give a time-frequency representation of a signal. One of them is the Short-Time Fourier Transform (STFT), which has been used frequently in many different disciplines. The disadvantage of STFT is that it only has a fixed resolution, which is determined by the "window function" used. For a better resolution in frequency, a wider window should be chosen whereas for a finer resolution in time a narrower window is required. However, when a good resolution is sought in both time and frequency, the STFT is not the ideal option.

To overcome the mentioned shortcoming of the STFT, a multi-resolution transform is required. One of the commonly used techniques in this context is the continuous wavelet transform (CWT). The CWT of a function $s(t)$ is given by

$$W(t,d) = \frac{1}{\sqrt{d}} \int_{-\infty}^{+\infty} s(\tau) w^*(\frac{\tau - t}{d}) d\tau \qquad (1)$$

where $w(t)$ is called the "mother wavelet" and the asterisk stands for operation of complex conjugate; d and t are the dilation and translation factors, respectively. By varying t and d, the window can be shifted in time and frequency. There are many families of mother wavelets proposed in the literature. The one that suits the application of load decomposition needs to have good frequency resolution for low frequencies and a good resolution in time for high frequencies. This is particularly important when the signal is the instantaneous power because the fundamental frequency is located around 120 Hz (or 100 Hz in a 50 Hz system) and a DC component is also present. Refer to Section IV-A for explanation. The S transform (ST) [22] is a perfect choice for this purpose. This transform has a frequency-dependent window size, which localizes the scalable Gaussian window dilations (d) and translations (τ). The ST of $s(t)$ is defined as:

$$S(t,f) = \int_{-\infty}^{+\infty} s(\tau) \, \frac{|f|}{\sqrt{2\pi}} \, \mathrm{e}^{-\frac{(t-\tau)^2 f^2}{2}} \, \mathrm{e}^{-i2\pi f\tau} \, \mathrm{d}\tau \qquad (2)$$

in which f is the frequency and $S(t,f)$ is the ST of $s(t)$. The ST has advantages over its competitors such as the STFT and the Wigner distribution function. It is shown in [22] that its competitors may fail to detect the high frequency contents of a signal while the ST perfectly detects them. A fast version of the ST was proposed in [23] and is easy to implement on a microprocessor.

The ST of a time series can be visualized in a 2-D graph with time on the horizontal axis, frequency on the vertical axis, and the magnitude of $S(t,f)$ coded into colors. This 2-D graph can be interpreted as an image. With this interpretation, the transient current corresponding to each load is mapped into a "photo" of that load. At this point, the problem of load recognition is transformed into the familiar problem of face recognition.

B. Derivation of Eigenloads

1) Principal Component Analysis: Assume a set of variables, N, which are possibly correlated. The Principal Component Analysis (PCA) is a technique to develop an orthogonal basis with minimum number of elements to represent N. Since some/all of the variables in N are correlated, it may be possible to represent these variables using a smaller number of uncorrelated variables. Consider a set of data of n single-column vectors $L_i \in \mathbb{R}^m$. The average feature ψ of this set can be calculated as:

$$\psi = \frac{1}{n}\sum_{i=1}^{n} L_i \tag{3}$$

The difference between each vector and the average is

$$\Phi_i = L_i - \psi \tag{4}$$

The PCA attempts to find n orthogonal vectors V_j and their corresponding eigenvalues λ_j that can uniquely span the space of all L_i. The eigenvectors defining this space can be calculated from the following covariance matrix:

$$C = \frac{1}{n}\sum_{i=1}^{n} \Phi_i \Phi_i^T = A\,A^T \tag{5}$$

where $A = [\Phi_1\, \Phi_2\, \ldots\, \Phi_n] \in \mathbb{R}^{m\times n}$. The eigenvectors of C, labeled as V_j, are the set of orthogonal basis for the data space. Some of the eigenvectors may be eliminated based on their associated eigenvalues. That is, eigenvectors associated with small eigenvalues can be eliminated since they contain negligible features (variances). Let all the remaining eigenvectors be placed in a matrix $E = [V_1\, V_2\, \ldots\, V_r]$, with r standing for the number of remaining eigenvectors. Any L_i can now be defined using a linear combination of the reduced eigenvectors:

$$w_i = \Phi_i^T\, E \tag{6}$$

in which $w_i \in \mathbb{R}^r$ is the vector of weights. To understand the concept, an example is given in the following.

Assume the following data is given:

$$L_1 = \begin{bmatrix}1\\2\end{bmatrix},\quad L_2 = \begin{bmatrix}2\\3.7\end{bmatrix},\quad L_3 = \begin{bmatrix}3\\5.5\end{bmatrix}$$

Then the average is

$$\psi = \begin{bmatrix}2\\3.73\end{bmatrix}$$

Subtracting the average from all L_i yields

$$\Phi_1 = \begin{bmatrix}-1\\-1.73\end{bmatrix},\quad \Phi_2 = \begin{bmatrix}0\\-0.03\end{bmatrix},\quad \Phi_3 = \begin{bmatrix}1\\1.77\end{bmatrix}$$

The covariance matrix can then be calculated as

$$C = \begin{bmatrix}\Phi_1 & \Phi_2 & \Phi_3\end{bmatrix}\begin{bmatrix}\Phi_1\\ \Phi_2\\ \Phi_3\end{bmatrix} = \begin{bmatrix}2 & 3.5\\ 3.5 & 6.13\end{bmatrix}$$

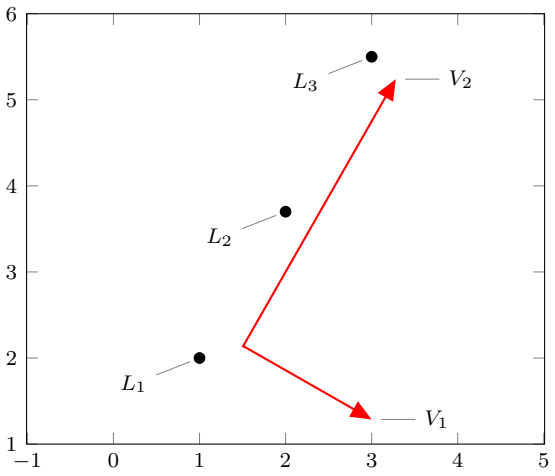

Figure 1. Illustration of Principal Component Analysis. V_1 and V_2 are scaled for proper representation.

The eigenvalues and eigenvectors associated with C are

$$V_1 = \kappa_1\begin{bmatrix}-0.8683\\0.4961\end{bmatrix}, V_2 = \kappa_2\begin{bmatrix}0.4961\\0.8683\end{bmatrix}$$

$$\lambda_1 = 0.0004, \lambda_2 = 8.1263$$

where $\kappa_1 \in \mathbb{R}$ and $\kappa_2 \in \mathbb{R}$ are scaling factors and are equal to 1 to obtain a normalized (unity) Euclidean norm. The contribution of each eigenvector in each L_i can be found by (6). Using these weights the vectors L_i can be reconstructed as follows:

$$\begin{aligned} L_1 &= 0.0084V_1 - 2.0011V_2 + \psi\\ L_2 &= 0.0000V_1 - 0.0333V_2 + \psi\\ L_3 &= 0.0081V_1 - 2.0300V_2 + \psi \end{aligned}$$

This is an exact representation of L_i. However, it can be seen from the eigenvalues (λ_1, λ_2) that the first eigenvector does not contain significant information and, thus, can be eliminated. By doing so, only one vector, i.e. V_2, would be sufficient to reconstruct a good approximation of the original vectors. The followings are the reconstructed vectors by only using V_2:

$$\hat{L}_1 = \begin{bmatrix}1.007\\1.996\end{bmatrix},\quad \hat{L}_2 = \begin{bmatrix}1.986\\3.708\end{bmatrix},\quad \hat{L}_3 = \begin{bmatrix}3.007\\5.496\end{bmatrix}$$

As can be seen, the error in the reconstructed vectors $\hat{L}_i$ is negligible.

The above example has a conceivable interpretation too. The vectors L_i are deliberately chosen close to the line $y = 2x$ in a plane. Regardless of the number of points, only one basis is sufficient to represent them, since x and y are almost linearly dependent in this case. This fact is illustrated in Fig. 1. Note that the length and position of the two eigenvectors can be chosen arbitrarily, as long as the directions are maintained.

2) Eigenloads: Assume that measurement data is available for n different load signatures, each with the same sampling frequency (f_s) and time interval ($t_{\max}$). This gives $m = f_s\, t_{\max}$ samples per measurement. The maximum frequency that can be detected in the signal is less than the sampling rate.

Applying the ST to the i^{th} measurement results in a 2-D array $S_i(t, f)$ containing the magnitudes of the transformation with time and frequency coordinates. It is possible to choose the resolution of the frequency axis to be equal to the resolution of the time axis. This way, the 2-D array $S_i(t, f)$ becomes an m by m square matrix.

Each matrix S_i is then rearranged into a single-column vector $L_i \in \mathbb{R}^{m^2}$. The PCA can then be applied to the set of L_i. Since $A = [\Phi_1\, \Phi_2\, \ldots\, \Phi_n] \in \mathbb{R}^{m^2 \times n}$, then the covariance matrix C is large (note that $C \in \mathbb{R}^{m^2 \times m^2}$) and is computationally expensive to conduct an eigenvalue analysis for. The method described in [24] avoids this problem (also used in [1]). Instead of finding the eigenvalues and eigenvectors of C, one can find those for $\Lambda = A^T A$, which is a n by n matrix. Conducting an eigenvalue analysis on a n by n matrix is much easier than an m^2 by m^2 one. Assume the eigenvectors of Λ to be U_j. The eigenvectors of C, denoted by V_j, can then be calculated as:

$$V_j = A\, U_j \tag{7}$$

The set of eigenvectors V_j are the orthogonal basis of the load signature space. For this reason, we call them the *eigenloads*. Some of the eigenloads may be eliminated based on their associated eigenvalues.

The eigenloads can be extracted from a library of load signatures. In this framework, load signatures form the feature space, or "load space". The eigenloads may not resemble an individual load signature and have no physical meaning. They contain the most significant features of loads that can be used to reconstruct all the load signatures.

Theoretically, the number of eigenloads to reconstruct all the signatures in the training set may be equal to the size of the training set. However, the number of eigenloads can be reduced to approximately reconstruct the signatures with fewer eigenloads. This reduces the computation and storage requirements of the algorithm, but may introduce a small error in the recognition part. Nonetheless, this error is negligible, as is shown in Section III. The following steps need to be taken to form a library of eigenloads:

1) Collect the load signatures and form the training set T.
2) Apply the ST to all the members in T.
3) Calculate the eigenloads using the transformed load signatures in T, as described in Section II-B2.
4) Keep the eigenloads with large eigenvalues (more significant) and form the library.

C. Recognizing a New Measurement

Once the library of eigenloads is formed, it can be used for near-real-time recognition of inputs. The recognition algorithm is summarized in the flowchart given in Fig. 2(a). The current and voltage waveforms can be obtained from a smart meter with some sampling rate, e.g., 10 kHz. As soon as a load is turned on/off, the detection algorithm shown in Fig. 2(b) captures the switching action, determines the load type using the recognition algorithm in Fig. 2(a), and updates the list of ON loads. If a load was previously ON and is now turned off, the algorithm is able to detect this action based on the decrease in the magnitude of the total current. Turning off a device reduces the total current magnitude. When a device is turned on, its current waveform is measured and the triggering signal is set to zero by subtracting the present window from the previous one. A similar procedure applies when a load is turned off.

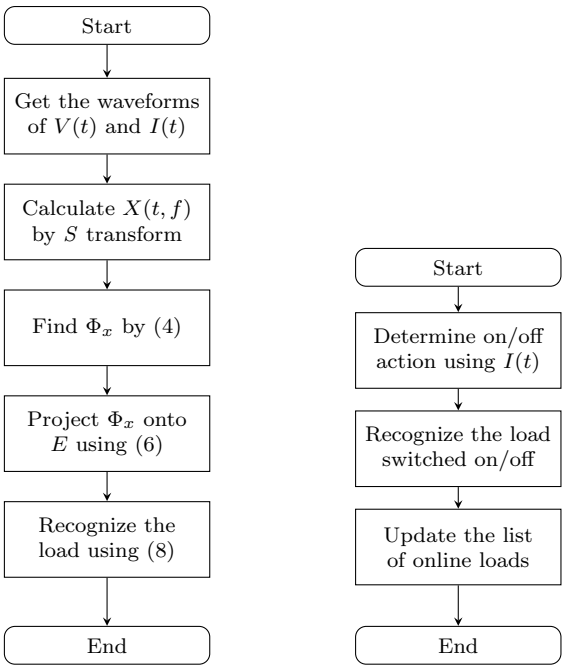

(a) Recognition (b) Detection

Figure 2. Flowchart of near-real-time load decomposition algorithm.

Once a new signal is received, its ST is calculated (X in Fig. 2(a)). Then the average feature ψ given by (3) is subtracted from X as in (4), denoted by Φ_x. The projection of Φ_x into E gives the weights w_x. The library of eigenloads contains the vector of weights w_i for all the loads in the training set. The recognition problem here is to compare the new vector w_x with the vectors in the library and determine the most similar signature. This can be done by, for example, using normalized vectors and then compare the angles between vector w_x and all other vectors w_i, i.e.:

$$\theta_i = \cos^{-1}\left(\frac{\vec{w_i}\,.\vec{w_x}}{\|\vec{w_i}\|\,\|\vec{w_x}\|}\right) \tag{8}$$

The smallest θ_i is the most similar load signature to the new measurement.

D. Load Classification

Most of loads have distinct signatures, which makes the recognition easy and accurate. However, there are loads that are of different type, but may have similar signatures. For instance, conventional electric heating appliances (without power electronic interfaces) may have similar current waveforms. Good examples are irons, heaters, ovens, electric kettles, electric rice cookers, electric hair curlers, and even incandescent lights. These types of loads are essentially resistive loads and have negligible reactive power. They also produce

negligible harmonics and, therefore, have similar signatures. Although one may not be able to detect the exact type of the load in such cases, it is still quite useful to be able to recognize the load as a member of a known family, e.g., resistive loads in this case.

The above discussion motivates the authors to give a more general direction to the load decomposition process. Instead of looking for specific loads, one may look for broader families of loads. To this end, a load classification for a typical residential customer is given in Table II. Besides its meaningful physical interpretation, this categorization is essentially driven by the eigenloads. When treating the load signatures as vectors defined by the weights obtained from (6), then the angles between these vectors given by (8) represent the similarities between the different signatures. By carefully choosing an appropriate threshold, the loads with similar transient characteristics can be clustered into a distinct group. Mathematically, loads i and j belong to the same load cluster if the following criterion is met:

$$|\theta_i - \theta_j| \leq \theta_{\text{th}} \tag{9}$$

A proper value for θ_{th} can be obtained by try-and-error. In this case, experience showed that $\theta_{\text{th}} = 10^\circ$ is a viable choice to avoid overlapping between the different subclasses. Based on this load classification, instead of categorizing a measurement as a specific load, the load identification algorithm categorizes the measurement under a broader family of loads. This is also a relaxation on the load identification algorithm and, thus, greater rates of success in the recognitions are achieved.

The proposed load decomposition algorithm is capable of identifying the loads under each subclass given in Table II. Further distinguishing between loads falling under the same subclass is not usually useful from the power utility point of view. For instance, a meat grinder and a vacuum cleaner may have similar signatures which makes them fall under the second subclass, i.e. medium-size induction motors (IM). From a load modeling perspective, however, it suffices to know they belong to the class of induction motors rather than the class of other appliances.

III. Laboratory Measurements

In this section, the application of the proposed framework is shown through real measurements. A number of electric devices were analyzed in the lab and their current and voltage waveforms were recorded for a period of a few seconds. The sampling frequency is 10 kHz. With this sampling rate, harmonics up to 1.0 kHz can be detected with high accuracy. A current probe and a voltage probe (differential probe) for measuring the corresponding quantities were attached to an oscilloscope. Furthermore, the measurements collected at the Carnegie Mellon University [25], which are freely available to the public under the name BLUED, were also used. In total, 46 measurements were available, from which 23 were chosen for building the eigenloads and the rest were left for testing.

Three examples of measurements and their STs are shown in Figs. 3-5. The figures illustrating the ST results are actually the contour visualization of square matrices with normalized elements. Some loads, such as the vacuum cleaner (induction motor) shown in Fig. 3, exhibit a fairly constant frequency content over time, while the magnitude of the current has a decaying component (inrush current). The instantaneous power of induction motors has a large DC component and a 120 Hz component decaying over time. Some loads have multiple stages from the starting moment to the steady state. The current waveform from a MAC laptop charger shown in Fig. 4(a), for example, has this characteristic. It shows higher frequency components in the middle stage and they start damping out after a few cycles. Some power electronic-driven loads draw a current rich in harmonics of different frequencies. The current waveform of a fluorescent lamp driven by an electronic ballast, shown in Fig. 5(a), has a low frequency envelope on top of the fundamental frequency. This feature produces a variety of frequency components in the instantaneous power, which are reflected in the ST shown in Fig. 5(b). The reason behind the existence of the even harmonics in the STs is briefly investigated in Section IV-A.

The 23 loads used to construct the eigenloads include incandescent lamps, fluorescent lamps (with magnetic and

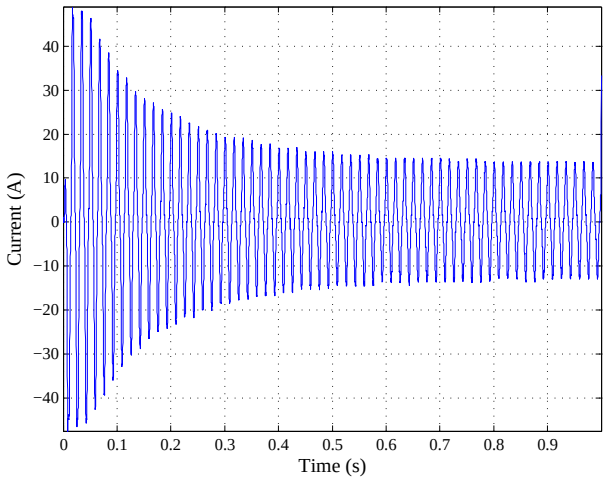

(a) Instantaneous current ($I(t)$)

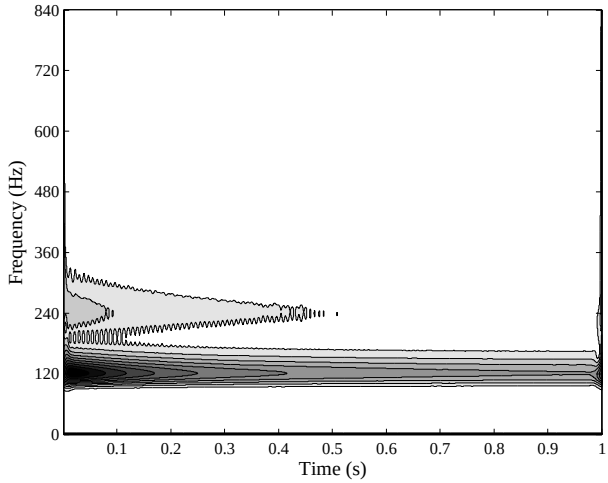

(b) S Transform ($S(t, f)$)

Figure 3. Current waveform of a vacuum cleaner and its S transform.

Table II
LOAD CLASSIFICATION FOR A TYPICAL RESIDENTIAL CUSTOMER

Class	No.	Subclass	Features	Examples
Motor	1	Small IM	Lagging PF	Fan
	2	Medium IM	Inrush current, lagging PF	Vacuum cleaner, AC
	3	Power electronic-driven IM	Non-sinusoidal	Washing machine, hand mixer
Resistive	4	Direct interface	Sinusoidal, unity PF	Incandescent light, heater
	5	Power electronic interface	Harmonics	Oven, iron
Fluorescent lamp	6	Magnetic ballast	Multi-stage starting, lagging PF	-
	7	Electronic ballast	Multi-stage starting, leading PF, harmonics	-
TV	8	CRT	Harmonics	-
	9	LCD-LED	Harmonics, leading PF	-
Electronic Cooker	10	Microwave oven	Multi-stage, harmonics	-
	11	Induction cooker	Multi-stage, harmonics	-
Electronics	12	Chargers	Multi-stage, harmonics	Laptop charger, phone charger
	13	Others	Harmonics	PC, DVD-player

electronic ballasts), hair drier, refrigerator, fan, a variety of induction motors, blender, meat grinder, vacuum cleaner, hand mixer, phone chargers, laptop chargers, electric shaver, personal computer, TV (LCD, LED, CTR), DVD player, iron, heater, induction cooker, hot plate, and microwaves. These loads cover most of the typical loads for a residential customer. Further analysis is to be done for commercial and

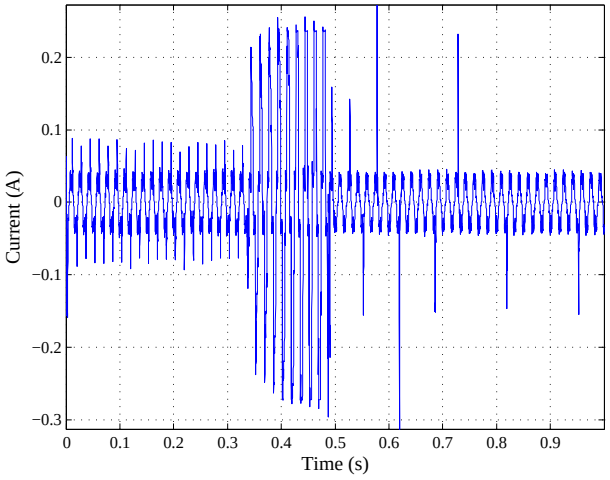

(a) Instantaneous current ($s(t)$)

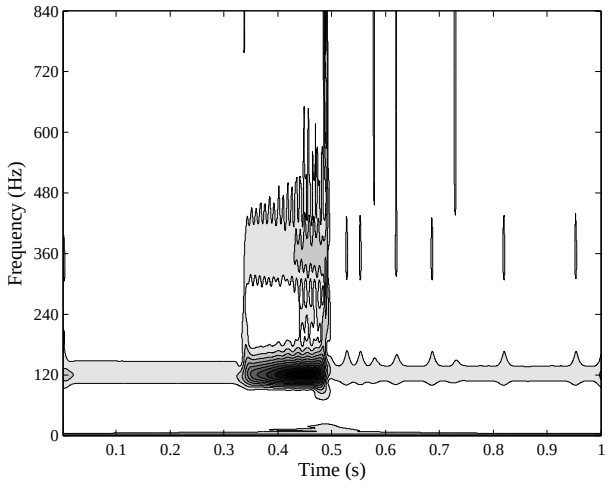

(b) S Transform ($S(t, f)$)

Figure 4. Current waveform of a MAC laptop charger and its S transform.

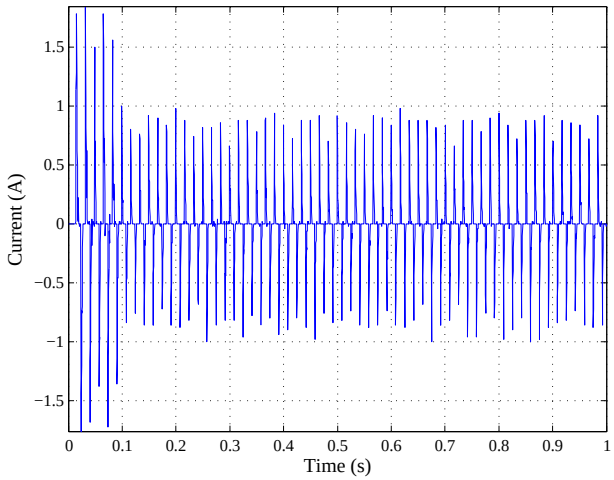

(a) Instantaneous current ($I(t)$)

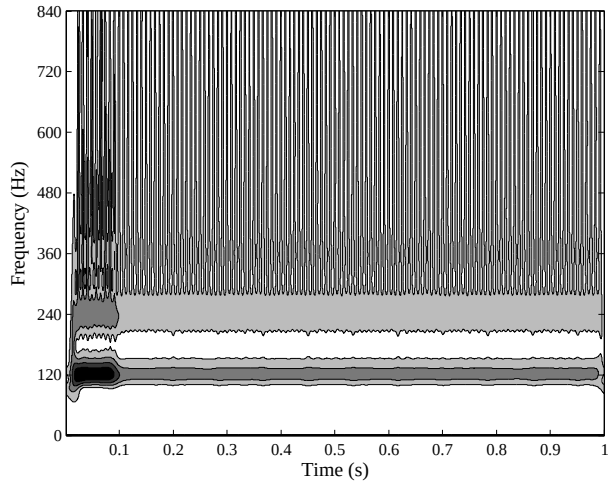

(b) S Transform ($S(t, f)$)

Figure 5. Current waveform of a T5 fluorescent lamp and its S transform.

industrial loads. The idea, however, is applicable to all type of consumers.

A. Evaluation of the Load Decomposition Mechanism

Based on the eigenvalue criterion, 10 eigenloads out of 23 were discarded, i.e. only 13 eigenloads are sufficient to form a basis for the load signatures space. This reduces the memory storage and processing requirements substantially. This fact is further discussed in Section IV-C. In order to test the proposed load decomposition approach, measurements for devices that were not present in the training set were used. The comparisons between the new measurements and the load subclasses in Table II are made using (8) in terms of angle differences. The results of these comparisons are depicted in Fig. 6. The outcomes of six tests are discussed here for illustration purposes. An LCD load manufactured by Samsung was used in the training set, while an LCD manufactured by ViewSonic with different ratings was used to test the algorithm. The results for this case are shown in Fig. 6(a). A hand mixer equipped with multiple stages, which was not used in the training set, was used at its lowest and highest power settings and the recognition algorithm was applied. The results are shown in Figs. 6(b) and 6(c). It should be noted that in its first power setting, the hand mixer is driven by power electronics and, hence, the current drawn from the network is not sinusoidal (Subclass 3). In its higher settings, however, the device draws a fairly sinusoidal current and, thus, resembles an induction motor (Subclass 2).

A heater equipped with a small fan, also not present in the training set, was tested and the results are shown in Fig. 6(d) (Subclass 4). A compact fluorescent lamp was tested which has slightly different waveforms than the T5 fluorescent lamps used in the training set. The recognition algorithm, as shown in Fig. 6(e), was still able to appropriately determine the closest load type (Subclass 7). A personal computer was also tested and the results are shown in Fig. 6(f), in which the algorithm categorizes this load under Subclass 13. The proposed algorithm also demonstrated a high rate of success in other laboratory tests, not presented here.

There is a trade-off between the number of eigenloads used and the accuracy of the recognition algorithm. Increasing the number of discarded eigenloads can save on memory storage and computation requirements, while potentially affecting the accuracy of the recognition process. For example, let us reconstruct the vacuum cleaner's ST using a reduced number of eigenloads. Figure 7 shows the changes in the ST when the number of eigenloads used (r) is continuously reduced. As can be seen, down to $r = 10$, the image is still close to the original one ($r = 23$). Beyond this point, however, the differences become noticeable. A good measure to compare the reconstructed image and the original image is the angle difference given by (8). This is done by setting the weights corresponding to the discarded eigenloads to zero in ω_i. This procedure was carried out for all the 23 loads and the results are shown in Fig. 8. As can be seen, by discarding up to 10 eigenloads, the difference between the original and reconstructed images remain within 10°. Therefore, 13 eigenloads

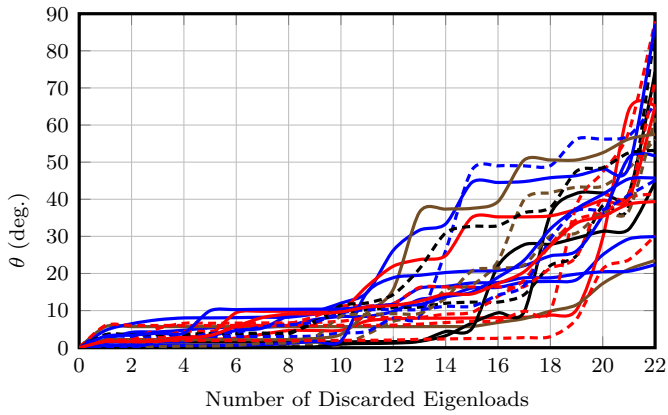

Figure 8. Differences between the original and reconstructed images with reduced number of eigenloads.

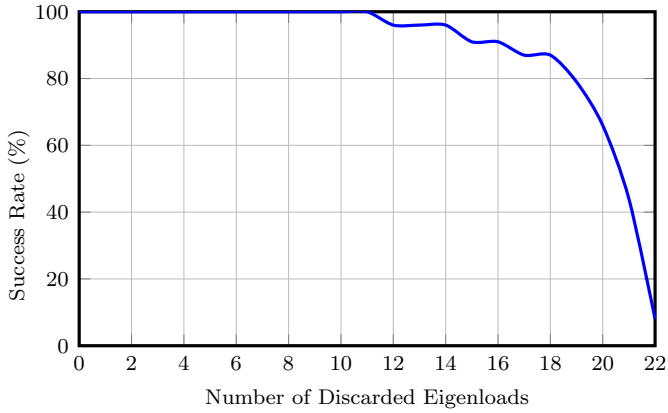

Figure 9. Rate of success in the recognition process versus the number of discarded eigenloads.

are found to be sufficient to define the load signature space.

The number of eigenloads used can affect the success rate in the recognition process. In order to show this, eignloads were discarded one after another and the recognition procedure was applied to all the test cases. The rate of success versus the number of eigenloads discarded is illustrated in Fig. 9. As can be seen, discarding up to 11 eigenloads did not affect the rate of success in the test cases. However, the rate of success is slightly dropped when more eigenloads are eliminated. By discarding 18 or more eigenloads, the rate of success is significantly deteriorated. Therefore, discarding 10 eigenloads keeps a balance between the accuracy and the computation and memory requirements of the proposed algorithm.

B. Robustness Against Noisy Measurements

In order to show the robustness of the proposed approach, the effect of noise on its performance is analyzed here. A random Gaussian noise with a zero-mean and a variance equal to 30% of the RMS value of current was added to the original current waveforms. For example, Fig. 10 shows the original current waveform and the noisy version for a LCD unit. The noisy measurements were used to perform the recognition process. The results are shown in Fig. 11(a). The

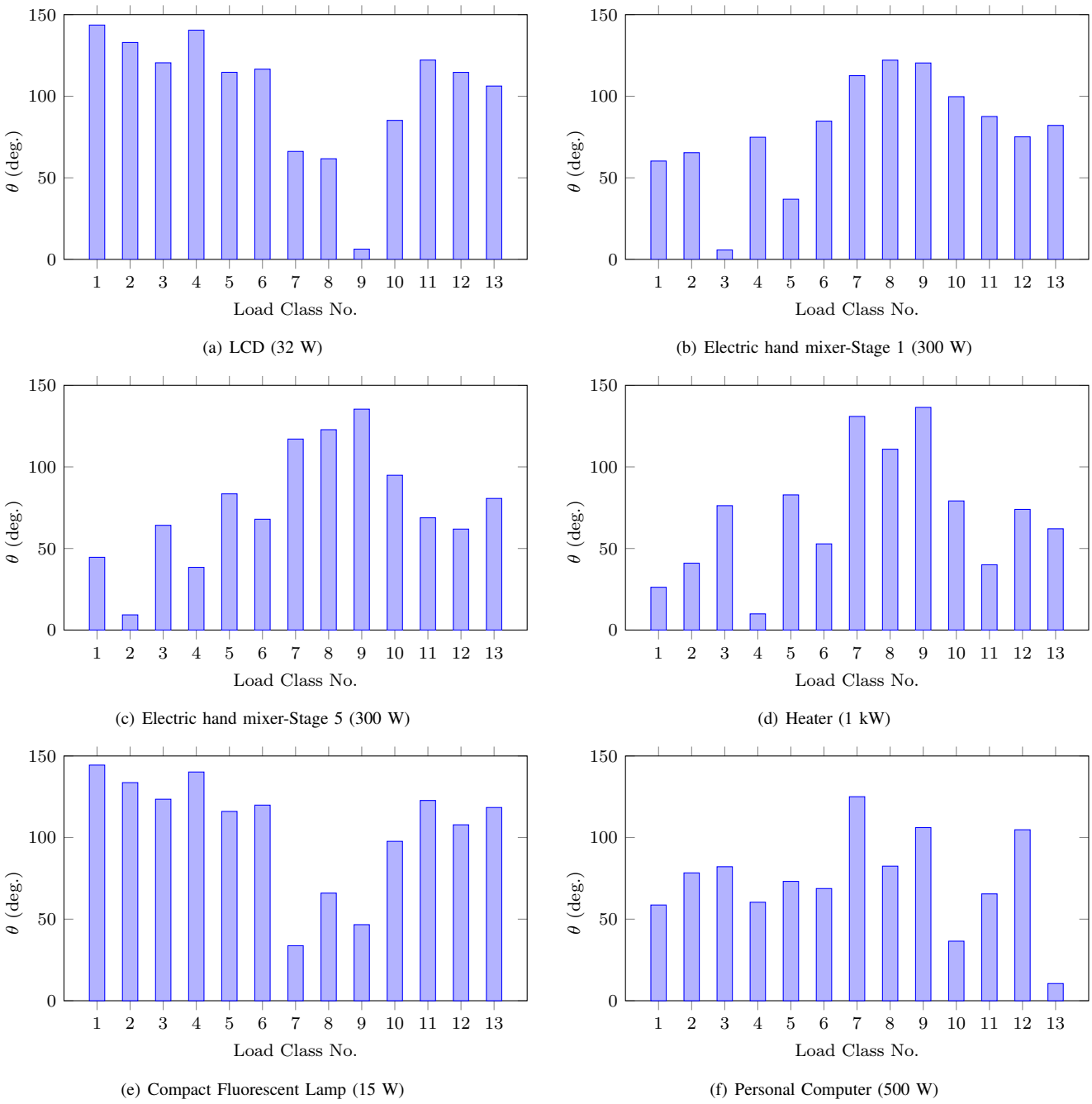

(a) LCD (32 W)

(b) Electric hand mixer-Stage 1 (300 W)

(c) Electric hand mixer-Stage 5 (300 W)

(d) Heater (1 kW)

(e) Compact Fluorescent Lamp (15 W)

(f) Personal Computer (500 W)

Figure 6. Results of recognition tests on devices not present in the training set (θ is defined by (8)).

same process was done for the hand mixer with the results shown in Fig. 11(b). These results show that the accuracy of the proposed approach is robust under noisy measurements. The main reason is that the ST filters the higher frequencies since the upper bound on the frequency components used in the training and recognition process is set to the fifteenth harmonic (900 Hz in a 60 Hz system).

IV. Discussion

A. Analytical Derivation of Instantaneous Power

The current waveform is a good choice for the load signature since each type of load, to some extent, has a distinct current waveform. However, as discussed earlier in Section II, the phase shift between the voltage and current waveforms (i.e., the power factor) would be lost if only the current waveform were used. For this reason, instantaneous power ($s(t)$), which is the point-wise multiplication of voltage and current signals, is used here. Assume a sinusoidal waveform of the voltage and a non-sinusoidal waveform of the current, represented by its truncated Fourier series:

$$V(t) = V_1 \sin(\omega t) \tag{10a}$$

$$I(t) = I_0 + \sum_{k=1}^{N} I_k \sin(k\omega t + \phi_k) \tag{10b}$$

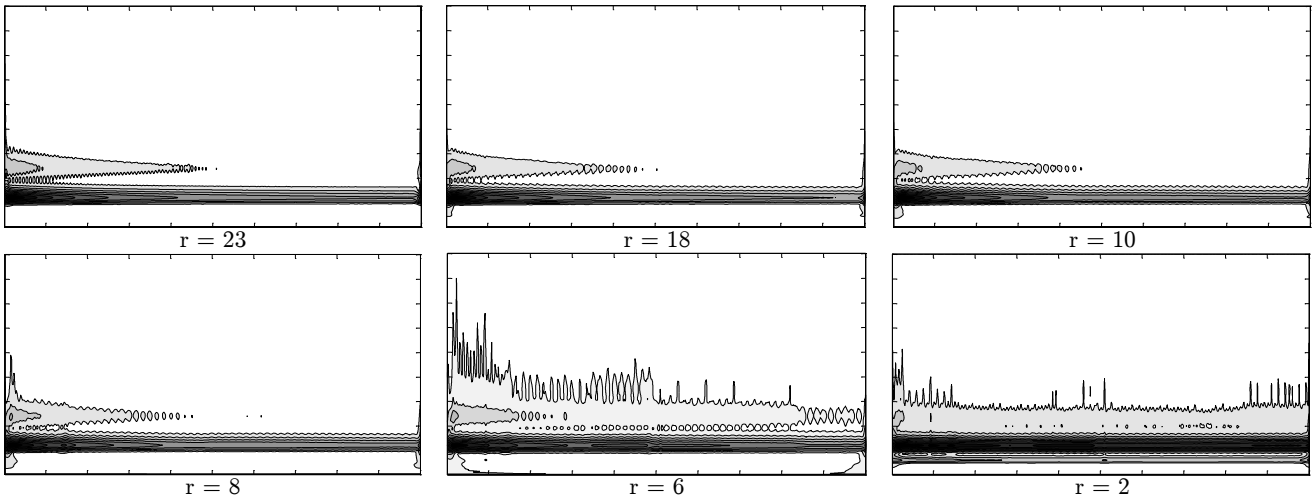

Figure 7. The S Transform of the vacuum cleaner reconstructed by a reduced number of eigenloads (r is the number of used eigenloads).

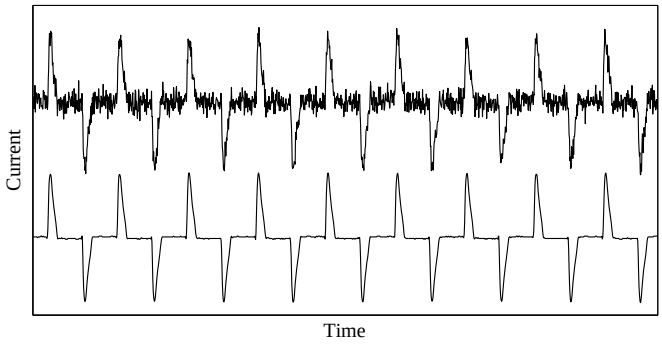

Figure 10. Current waveforms of a LCD; bottom: original; top: noisy by a random Gaussian noise with a zero-mean and 30% of RMS value of current as its variance.

With these assumptions, $s(t)$ can be calculated as:

$$s(t) = I_0 V_1 \sin(\omega t) + \sum_{k=1}^{N} \frac{V_1\, I_k}{2} \big[\cos\big((k-1)\omega t + \phi_k\big) - \cos\big((k+1)\omega t + \phi_k\big)\big] \quad (11)$$

Consider, for example, that the current has only the first and the third harmonics (e.g., induction motors). In this case, $s(t)$ would have a DC component as well as the second and the fourth harmonics of the fundamental frequency. This simple analysis explains the presence of the even harmonics in the STs. In some cases, e.g., some power electronic-driven loads, the current drawn by the device may have a DC component or some even harmonics. Under such circumstances, $s(t)$ has a frequency content of both odd and even multiples of the grid frequency.

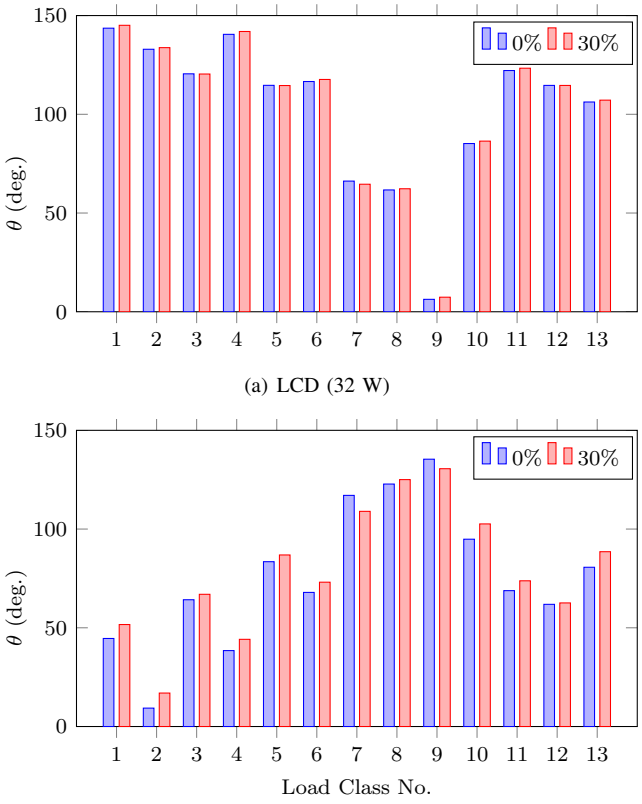

(a) LCD (32 W)

(b) Electric hand mixer-stage 5 (300 W)

Figure 11. Effect of noise on recognition accuracy. A Gaussian noise with zero-mean and a variance of 30% of the RMS value of current is added to the original current waveform.

B. Applications

In terms of applications, load composition at the customer level is useful in the following aspects.

1) Tariff Policies: Multi-rate tariff for energy consumption has been used as a tool for demand-side management and/or energy saving purposes. This system of energy tariff is usually based on time-of-use or level of energy consumption. In the first case, the price per kWh is different in defined time intervals, usually more expensive during the peak time and cheaper in light load periods. In the second case, there are thresholds on the kWh consumption per month and when each one of those thresholds is exceeded, the price per kWh increases. In order to design an efficient tariff system in both cases, an understanding

of the customer behavior is useful. If the components of load used by the customer are known to the utility, it is then possible to estimate how much of this load is potentially responsive to a price signal or other similar policies. For instance, if the peak load occurs around 7 pm, and the measurements show that many households use the washing/drying machines at this time, then there is a possibility to shift part of the load by intensifying the customers. It is then a good measure to estimate the effectiveness of a tariff policy before applying it. More discussion on this topic can be found in, e.g., the EPRI report on customer behavior [26].

2) Customer Benefits: By carefully studying the customer's electricity consumption, it is possible to provide useful feedback on possible ways to conserve energy. For example, by monitoring the consumption of each appliance, inefficient appliances can be identified. A cost-benefit analysis can be provided on replacing the inefficient appliance with a better one. Also, suggestions can be given on using particular devices during light-load periods to save on electricity bill.

3) Short-Term Load Forecasting: The average load is sensitive to several factors including ambient temperature, sun light, grid voltage and frequency, etc. There are some specific components of load that are more sensitive to the mentioned factors than others. For example, if temperature increases above the expected values, the air conditioners need to work more than expected. If the portion of load corresponding to air conditioning and the sensitivity of this type of load to temperature are known, then a good estimation of load deviation from the forecast can be derived. The load sensitivity to temperature is referred to as temperature elasticity in [27], in which the effects of weather condition on load is thoroughly discussed. Moreover, the load composition estimation can be used in building-level demand response in the distribution system market [28].

4) Near-Real-Time Load Modeling: In distribution system level, near-real-time control actions may be applied by the DMS. These actions include volt-VAR control and optimization (VVO) [29] and voltage-dependent power flow analysis [30], which require a good estimation of load response to voltage variations. A good voltage-dependent load model is beneficial for such cases. In transmission system level, near-real-time dynamic analysis such as transient and voltage stability assessments require a good estimation of load model at each substation. The aggregated load composition at the substation can be used to build an accurate model of load static and dynamic behavior seen from the transmission system [31].

C. Implementation Aspects

Additional values can be added to the present advanced metering infrastructure by implementing the proposed load decomposition technique at the smart meters level. Load composition can be sent along with the electricity consumption and voltage level to the control center, where the received data is stored and analyzed. In order to implement the proposed algorithm at the smart meters, the memory storage and computation requirements of the algorithm should not exceed the capabilities of available hardware.

The largest memory requirement of the algorithm is pertained to the library of eigenloads. It was shown in Section III that 13 eigenloads are sufficient to have satisfactory results. Also, the resolution of the images representing each eigenload can be reduced to save storage requirements, without affecting the accuracy of the results. Based on experience, a resolution of 500×500 is sufficient. Using this resolution and assuming a double-precision floating-point format, each eigenload requires $500 \times 500 \times 8$ bytes of memory storage. For 13 eigenloads, this adds up to 26 Mb. This is well within the capability of external RAMs (random access memory) available for FPGAs (field-programmable gate array). An example is Stratix V from Altera that works with DDR3 memories at 1,866 Mbps.

The highest computation-intense part of the algorithm is the calculation of the *S* Transform (ST) of a measurement. The discrete ST proposed in [23] has a computational complexity of $\mathcal{O}(N \log N)$, where N is the number of data points in the signal. This is equivalent to the complexity of the Fast Fourier Transform [23], which has been previously implemented in many hardware platforms. The structure of the ST given in (2) is in such a way that each point in the time-frequency plane can be calculated independently. Therefore, efficient parallel implementation of the ST can be realized on common microprocessors such as FPGAs. A good example of real implementation of the ST on FPGA is [32].

D. Limitations

Since the proposed method works based on the transient features of loads, it does not work properly when two loads of different types are switched on simultaneously. This occurs because the algorithm assumes the captured transient belongs to one single type of load and, therefore, its time-frequency representation stands for a particular load. Nonetheless, this is a rare event that two loads of different types are turned on simultaneously in a household.

Another limitation of the proposed algorithm is that it is unable to further distinguish between loads with similar signatures but different applications. For example, most of the resistive loads have similar signatures, while they may have different functions. For the targeted applications mentioned in Section IV-B, the resolution in the load composition provided by Table II is sufficient.

The proposed method requires measurements with relatively high sampling rates. Although the present data available from the smart meters has usually low sampling rates, the internal process in the smart meter itself occurs at much higher sampling rates. There is a great potential for implementing the proposed method at the smart meter and transmitting the load composition along with power consumption.

V. Conclusion

A framework for load decomposition at the smart meter level was proposed here which is applicable for load disaggregation in distribution systems. Instead of trying to recognize each individual load, the proposed framework categorizes the loads into major classes, each containing loads with distinct features. Only the load composition, which can be coded into

a few numbers, needs to be transmitted to the control center. This requires minimal amount of data transmission and the present communications technology for smart meters suffices. All the decomposition process is done at the smart meters. Therefore, the amount of data received by the control center is manageable. The proposed approach is robust against noisy measurements. The main contributions of this paper are as follows:

- A time-frequency representation of measurements is chosen as the load signatures.
- The concept of eigenloads, as the basis for the load signature space, is created.
- A framework for load decomposition based on the eigenloads concept is proposed.
- Residential loads are categorized into subclasses with physical and theoretical interpretations.
- Applications for the load composition data are established.

In undergoing work, the authors used the load composition data to build an accurate model of load representing its voltage dependence at near-real-time. This is useful for the realization of many applications within the distribution management system (DMS), especially volt-VAR optimization (VVO).

REFERENCES

[1] M. A. Turk and A. P. Pentland, "Face recognition using eigenfaces," in *IEEE CS Conf. CVPR'91*. IEEE, 1991, pp. 586–591.

[2] C. W. Gellings and R. W. Taylor, "Electric load curve synthesis-a computer simulation of an electric utility load shape," *IEEE Trans. Power Appar. Syst.*, vol. PAS-100, no. 1, pp. 60–65, Jan. 1981.

[3] G. W. Hart, "Nonintrusive appliance load monitoring," *Proceedings of the IEEE*, vol. 80, no. 12, pp. 1870–1891, 1992.

[4] S. Drenker and A. Kader, "Nonintrusive monitoring of electric loads," *IEEE Comput. Appl. Power*, vol. 12, no. 4, pp. 47–51, 1999.

[5] C. Laughman, K. Lee, R. Cox, S. Shaw, S. Leeb, L. Norford, and P. Armstrong, "Power signature analysis," *IEEE Power and Energy Magazine*, vol. 1, no. 2, pp. 56–63, 2003.

[6] H. Y. Lam, G. S. K. Fung, and W. K. Lee, "A novel method to construct taxonomy electrical appliances based on load signatures," *IEEE Trans. Consumer Elect.*, vol. 53, no. 2, pp. 653–660, 2007.

[7] T. Hassan, F. Javed, and N. Arshad, "An empirical investigation of V-I trajectory based load signatures for non-intrusive load monitoring," *IEEE Trans. Smart Grid*, vol. 5, no. 2, pp. 870–878, Mar. 2014.

[8] W. L. Chan, A. T. P. So, and L. L. Lai, "Harmonics load signature recognition by Wavelets transforms," in *Int. Conf. Elec. Utility Dereg. Restruc. Power Tech.* IEEE, 2000, pp. 666–671.

[9] J. Froehlich, E. Larson, S. Gupta, G. Cohn, M. Reynolds, and S. Patel, "Disaggregated end-use energy sensing for the smart grid," *IEEE Pervasive Computing*, vol. 10, no. 1, pp. 28–39, 2011.

[10] Z. Guo, Z. Wang, and A. Kashani, "Home appliance load modeling from aggregated smart meter data," *IEEE Trans. Power Syst.*, vol. 30, no. 1, pp. 254–262, Jan. 2015.

[11] M. Dong, P. C. Meira, W. Xu, and W. Freitas, "An event window based load monitoring technique for smart meters," *IEEE Trans. Smart Grid*, vol. 3, no. 2, pp. 787–796, 2012.

[12] A. G. Ruzzelli, C. Nicolas, A. Schoofs, and G. M. P. O'Hare, "Real-time recognition and profiling of appliances through a single electricity sensor," in *7th Annual IEEE Conf. SECON*, 2010, pp. 1–9.

[13] M. Figueiredo, A. De Almeida, and B. Ribeiro, "Home electrical signal disaggregation for non-intrusive load monitoring (NILM) systems," *Neurocomputing*, vol. 96, pp. 66–73, 2012.

[14] M. L. Marceau and R. Zmeureanu, "Nonintrusive load disaggregation computer program to estimate the energy consumption of major end uses in residential buildings," *Energy Conv. Man.*, vol. 41, no. 13, pp. 1389–1403, 2000.

[15] L. Farinaccio and L. Zmeureanu, "Using a pattern recognition approach to disaggregate the total electricity consumption in a house into the major end-uses," *Energy and Buildings*, vol. 30, no. 3, pp. 245–259, 1999.

[16] P. Ducange, F. Marcelloni, and M. Antonelli, "A novel approach based on finite-state machines with fuzzy transitions for nonintrusive home appliance monitoring," *IEEE Trans. Indust.l Inf.*, vol. 10, no. 2, pp. 1185–1197, May 2014.

[17] H.-H. Chang, K.-L. Chen, Y.-P. Tsai, and W.-J. Lee, "A new measurement method for power signatures of nonintrusive demand monitoring and load identification," *IEEE Trans. Ind. Appl.*, vol. 48, no. 2, pp. 764–771, 2012.

[18] H.-H. Chang, L.-S. Lin, N. Chen, and W.-J. Lee, "Particle-swarm-optimization-based nonintrusive demand monitoring and load identification in smart meters," *IEEE Trans. Ind. Appl.*, vol. 49, no. 5, pp. 2229–2236, Sept 2013.

[19] H. Chang, K. Lian, Y. Su, and W. Lee, "Power spectrum-based wavelet transform for non-intrusive demand monitoring and load identification," *IEEE Trans. Ind. Appl.*, 2014.

[20] J. Liang, S. K. K. Ng, G. Kendall, and J. W. M. Cheng, "Load signature study—Part I: Basic concept, structure, and methodology," *IEEE Trans. Power Del.*, vol. 25, no. 2, pp. 551–560, Apr. 2010.

[21] ——, "Load signature study—Part II: Disaggregation framework, simulation, and applications," *IEEE Trans. Power Del.*, vol. 25, no. 2, pp. 561–569, Apr. 2010.

[22] R. G. Stockwell, L. Mansinha, and R. P. Lowe, "Localization of the complex spectrum: the S transform," *IEEE Trans. Signal Proc.*, vol. 44, no. 4, pp. 998–1001, Apr. 1996.

[23] R. A. Brown and R. Frayne, "A fast discrete S-transform for biomedical signal processing," in *30th Ann. Int. Conf. Eng. Med. Bio. Society*. IEEE, 2008, pp. 2586–2589.

[24] M. Turk and A. Pentland, "Eigenfaces for recognition," *Journal of cognitive Neuroscience*, vol. 3, no. 1, pp. 71–86, 1991.

[25] K. Anderson, A. Ocneanu, D. Benitez, D. Carlson, A. Rowe, and M. Berges, "BLUED: a fully labeled public dataset for Event-Based Non-Intrusive load monitoring research," in *2nd KDD Workshop on Data Mining Applications in Sustainability*, Beijing, China, Aug. 2012.

[26] B. Neenan, "Quantifying the impacts of time-based rates, enabling technology, and other treatments in consumer behavior studies," EPRI, Protocols and Guidelines, Jul. 2013.

[27] C. Crowley and F. L. Joutz, "Weather effects on electricity loads: Modeling and forecasting," The George Washington University, Tech. Rep., Dec. 2005.

[28] D. He, W. Lin, N. Liu, R. G. Harley, and T. G. Habetler, "Incorporating non-intrusive load monitoring into building level demand response," *IEEE Trans. Smart Grid*, vol. 4, no. 4, pp. 1870–1877, Dec. 2013.

[29] H. Ahmadi, J. R. Martí, and H. W. Dommel, "A framework for volt-VAR optimization in distribution systems," *IEEE Trans. Smart Grid*, to be published.

[30] J. R. Marti, H. Ahmadi, and L. Bashualdo, "Linear power flow formulation based on a voltage-dependent load model," *IEEE Trans. Power Del.*, vol. 28, no. 3, pp. 1682–1690, Jul. 2013.

[31] IEEE Task Force, "Load representation for dynamic performance analysis of power systems," *IEEE Trans. Power Syst.*, vol. 8, no. 2, pp. 472–482, May 1993.

[32] B. Biswal, P. K. Dash, and M. Biswal, "Time frequency analysis and FPGA implementation of modified S-Transform for de-noising," *Int. J. Signal Proc. Image Proc. Pattern Recog.*, vol. 4, no. 2, pp. 119–136, Jun. 2011.

Hamed Ahmadi (S'12) received the B.Sc. and M.Sc. degrees in electrical engineering from the University of Tehran in 2009 and 2011, respectively, and is currently a Ph.D. candidate in electrical power engineering at the University of British Columbia, Vancouver, BC, Canada. His research interests include distribution systems analysis, optimization algorithms, power system stability and control, smart grids, and high voltage engineering.

José R. Martí (M'80-SM'01-F'02) received the Electrical Engineering degree from Central University of Venezuela, Caracas, in 1971, the Master of Engineering degree in electric power (M.E.E.P.E.) from Rensselaer Polytechnic Institute, Troy, NY, in 1974, and the Ph.D. degree in electrical engineering from the University of British Columbia, Vancouver, BC, Canada in 1981. He is known for his contributions to the modeling of fast transients in large power networks, including component models and solution techniques. Particular emphasis in recent years has been the development of distributed computational solutions for real-time simulation of large systems and integrated multisystem solutions. He is a Professor of electrical and computer engineering at the University of British Columbia and a Registered Professional Engineer in the Province of British Columbia, Canada.